Dielectric behaviour of Ni^{+2} substituted Cu Co Nanocrystalline Spinel Ferrite Material

A.M. Tamboli[1*], S.M. Rathod[3], Gulam Rabbani[2]

[1]*Department of Electronic Science, Poona College, Camp, Pune-411 001 INDIA.*
[2]*Department of Physics and Electronics, Maulana Azad College, Aurangabad-431 001 INDIA*
[3]*Department of Physics, Abasaheb Garware College, Pune- 411 004 INDIA*

Abstract: *Herein, the dielectric properties such as permittivity (real part ε' and imaginary part ε") and dielectric loss tangent (tan δ) are reported for the series [Ni_x Cu(constant) $Co_{0.8-x}$ Fe_2O_4] where constant=0.2 with x=0.2, 0.4 and 0.6 of ferrites, prepared by Sol-Gel auto-combustion technique by using high purity metal nitrate and citric acid as a catalyst. The variation in the real part (ε') of dielectric constant , imaginary part (ε") of dielectric constant and dielectric loss tangent (tan δ) are studied at room temperature in the frequency range of 100 Hz to 5 MHz. Structural characterization of the annealed samples was done with the help of X-ray diffraction method. The particle size and single phase formation of $NiCuCoFe_2O_4$ ferrite was confirmed by X-ray diffraction analysis and TEM. The particle size of prepared sample was confirmed by Scherer's formula. The effect on Particle size (t) and lattice constant (Å) is observed due to substitution of Ni^{2+} in Cu Co. The digital LCR meter is used to obtain the magnetic properties of prepared pallets. The variations in the structural and dielectric properties of the prepared ferrite material are discussed.*
Keywords: *Digital LCR, FT-IR, Sol-gel auto-combustion, TEM, X-ray diffraction.*

I. Introduction

Due to very different properties of ferrite material especially in electric, di-electric and magnetic properties that are sensibly different from the properties of the bulk materials, ferrite nanoparticle are popular in various fields of electronics and communication Engineering. Ferrite nanoparticles are very use full in the area where minimization of magnetic loss is important and magnetic field dependent properties plays very important role.

Ferrite nanoparticles are having very high electrical resistivity and due to this ferrite perform a better response at high frequencies. Ferrite is used as best core material in the transformers and switch mode power supply for frequencies from few kHz to a few MHz. Ferrite is having high stability, low cost, light weight and lowest volume therefore it is more popular. These are intensively studied due to their technological applications in microwave industries such as Radar Absorbing Material (RAM), satellite communication, microwave dark room and protection of living animals from the harm of microwave [1–14].

II. Experimental

2.1 Synthesis

The high purity AR grade ferric nitrate [$Fe(NO_3)_3.9H_2O$)], Copper nitrate [$Cu (NO_3)_2 .6H_2O$], Nickel nitrate [$Ni(NO_3)_2.6H_2O$],Cobalt nitrate [$Co(NO_3)_2.6H_2O$], citric acid ($C_6H_8O_7$), ammonium hydroxide solution (NH_4OH) were used to prepare the series [Ni_x Cu(constant) $Co_{0.8-x}$ Fe_2O_4] where constant=0.2 with x=0.2, 0.4 and 0.6 of ferrite nanoparticles by sol-gel auto combustion synthesis technique. In this chemical process Citric acid was used as a Fuel. These nitrates and citric acid were weighed accurately to have proper stoichiometric proportion required in the final product and all metal nitrates are dissolved in deionized water to form mixed solution. The mixed solutions of all the chemicals were stirred by using magnetic stirrer until the homogeneous solution is obtained. During the stirring process ammonium hydroxide solution was added drop by drop to obtain pH of 7. The mixed solution was simultaneously heated at 100 °C for 3 to 4 h to form sol. The transparent sol was heated at 120°C for 2 h for removal of water. The sol turns into a viscous brown gel. The temperature of the gel was further increased up to 150 °C, after some time combustion of the gel takes place and fine powder of [Ni_x Cu(constant) $Co_{0.8-x}$ Fe_2O_4] ferrite nanoparticle was obtained. The powder was dried and annealed at 400 °C for 4h in furnace having super kanthal ($MoSi_2$) heating elements and alumina insulation boards as chamber walls. The pallets of sample are prepared by using binder polyvinyl alcohol (PVA) and it was pressed at 60 kg/cm³ for one min and was dried and annealed at 200 °C for 2hours.The diameter of pallet is 10mm and thickness is 2mm. Three ferrite materials represented by the symbol A, B, and C are [($Ni_{.0.2}$ $Cu_{.0.2}$ $Co_{0.6}$) Fe_2O_4], [($Ni_{.0.4}$ $Cu_{.0.2}$ $Co_{.0.4}$) Fe_2O_4] and [($Ni_{.0.6}$ $Cu_{.0.2}$ $Co_{0.2}$) Fe_2O_4] respectively.

2.2 Characterization

The phase analysis and gross structural analysis is done by using X-ray diffractometer (Cu Kα_1 radiation=1.5418 Å) and confirmation of single phase spinal structure is done. The average particle size of prepared powder has been calculated using Scherrer formula

t = 0.9 λ /β cos θ

Where; □ = Wave length of X-rays.

t = Particle size.

θ = Bragg's angle.

β = Full Width Half Maxima of the recorded peak θ and it is corrected for
   instrumental broadening.

The lattice parameter (a) is calculated from X-ray diffraction data by using formula $1/d^2 = 1/a^2 * (h^2 + k^2 + l^2)$. It is observe that Average Grain Size t (nm) and Lattices Constant a (Å) decreases with increase of Ni^{2+} substitution of in Cu Co as shown in Table 1.

The dielectric constant (ε') , dielectric loss tangent (tan δ) and AC conductivity (σ_{ac}) of prepared samples were measured in the frequency range of 100 Hz to 5 MHz by using digital LCR meter of precision impedance analyser at room temperature. The data of digital LCR meter provides the information of frequency (f), Series Capacitance (Cs), Parallel Capacitance (Cp), Quality factor (Q) , by using the this date along with thickness of pellet, d=0.002 meter, Diameter of pellet= 10 millimetre and Area of pellet = π r^2 = 3.14*.005*.005 $meter^2$=0.0000785 $meter^2$, the calculations for dielectric constant (ε') , imaginary part (ε") of dielectric constant and dielectric loss tangent (tan δ) are completed by using the following equations. The logarithm of frequency (Log_{10} f) is taken in to consideration while plotting the graph of (Log_{10} f) verses any other parameter.

Dielectric constant (Real Part) = έ = Cp*d/ε_0*A

Dielectric constant (Imaginary Part) = ε″ = (tan δ)* ε'

Dielectric loss tangent= (tan δ) = 1/Q = ε″ / ε'

III. Results and Discussions

3.1 Structural analysis

The XRD pattern of as-synthesized ferrite material of [($Ni_{.0.2}$ $Cu_{.0.2}$ $Co_{0.6}$) Fe_2O_4], [($Ni_{.0.4}$ $Cu_{.0.2}$ $Co_{0.4}$) Fe_2O_4], [($Ni_{.0.6}$ $Cu_{.0.2}$ $Co_{0.2}$) Fe_2O_4] is shown in Fig.1. The highest intensity peaks in all three specimens are observed at (311) and other peaks (220), (400), (422) and (440). The average grain (crystallite) size for all the composites is calculated using Scherer's formula with respect to the high intense peak plane (311) and Lattices Constant a (Å) is calculated by using the formula $1/d^2 = 1/a^2 * (h^2 + k^2 + l^2)$. It is observed that due to the increase concentration of Ni^{2+} ions in Cu Co the Bragg's angle shifts towards higher angle and thereby interplaner spacing's (d) values decreases. The grain (crystallite) size for all the composites is found in the range of 28.45 nanometer to 22.52 nanometer. The XRD pattern contains no secondary peaks and it gives the confirmation about pure spinal structure of sample.

The lattice constant is found to decrease with increase in Ni^{2+} concentration x. The variations in lattice constant as a function of Nickel concentration x can be understood on the basis of the ionic radius of the substituted cations. Since the ionic radius of Ni^{2+} ions (0.69Å) is less than that of Co^{2+} ions (0.72Å), the substitution is expected to decrease the lattice constant with increase in nickel concentration x . When the smaller nickel ions enters the lattice unit cell expands while preserving overall symmetry this is true as long as the lattice constant decreases with substituent concentration. The values of lattice constant obtained from XRD data for varying nickel concentration x are given in Table 1. It can be seen from TABLE 1.that, the lattice constant decreases linearly with increase of nickel concentration x and obeys Vegard's law [15-20].

The TEM images shown in Fig. 2 for x=0.2 and x=0.4 gives the confirmation about decrease in the particle size and it is found in the range of 22 nanometer to 28 nanometer due to substitution of Ni^{2+} concentration x.

3.2 Dielectric properties

The effect of Ni^{2+} concentration x on the dielectric properties of [($Ni_{.0.2}$ $Cu_{.0.2}$ $Co_{0.6}$) Fe_2O_4], [($Ni_{.0.4}$ $Cu_{.0.2}$ $Co_{0.4}$) Fe_2O_4], [($Ni_{.0.6}$ $Cu_{.0.2}$ $Co_{0.2}$) Fe_2O_4] have been studied by using LCR meter (impedance analyzer) in frequency range of 100 Hz–5 MHz. The Fig. 3 shows the variation in the dielectric constant (έ) with increase in the frequency and it is observed that dielectric properties of spinel ferrite samples rapidly decreases at lower frequencies and remains constant at higher frequencies. The Fig. 4 shows that dielectric loss (tan δ) also decreases at low frequency. The Fig. 5 shows that the Imaginary Part of Dielectric constant (ε″) also decreases at low frequency. Similar results were observed by several other investigations [21-31]. The values of the dielectric constant and dielectric loss of the samples are listed in TABLE 2.

According to Koop's the decrease in dielectric constant for increase in frequency can be expressed by considering the solid as composed of well conducting grains which is separated by the poorly conducting grain

boundaries**.** According to Koop's, at lower frequencies, the resistivity is high and the principal effect is of the grain boundaries (low resistivity regions). Therefore, the energy required for electron hopping between Fe^{2+} and Fe^{3+} at the grain boundaries is higher and the energy losses (tan δ and ε″) are larger[32-33].

The rapid decrease of dielectric constant at lower frequencies is explained on the basis of space charge polarization. According to Maxwell and Wagner two-layer model, the space charge polarization is produced in a di-electric material due to the presence of higher conductivity phases (grains) in the insulating matrix (grain boundaries). When an external electric field is applied, the electrons reach the grain boundary through hopping. If the resistance of the grain boundary is high, the electrons pile up at the grain boundaries and produces polarization. This is called space charge polarization. The assembly of space charge carriers in a dielectric takes a finite time to line up their axes parallel to the alternating electric field. If the frequency of the field reversal increases, a point is reached where the space charge carriers cannot keep up with the field and the alternation of their direction lags behind that of the field .The FT-IR peaks at 536.114 cm^{-1} , 524.643 cm^{-1} and 532.257 cm^{-1} gives the confirmation of Fe$_2$O$_4$[34-41].

IV. Figures and Tables

Table 1: Variation of lattice constant a (Å) and Particle size (t) of Ni $_x$ Cu $_{0.2}$ Co $_{0.8-x}$ Fe$_2$O$_4$

[Ni$_x$ Cu(constant) Co$_{0.8-x}$], Cu=constant=0.2		
x	Grain Size t (nm)	Lattices Constant a (Å)
For x=0.2	28.45	8.4175
For x=0.4	25.89	8.3737
For x=0.6	22.52	8.3635

Table 2: Variation of Dielectric Constant and Dielectric loss of Ni $_x$ Cu $_{0.2}$ Co $_{0.8-x}$ Fe$_2$O$_4$.

[Ni$_x$ Cu(constant) Co$_{0.8-x}$], Cu=constant=0.2		
X	Dielectric Constant	Dielectric loss
For X=0.2	52.9070	0.701638
For X=0.4	40.3944	0.523854
For X=0.6	31.1225	0.255394
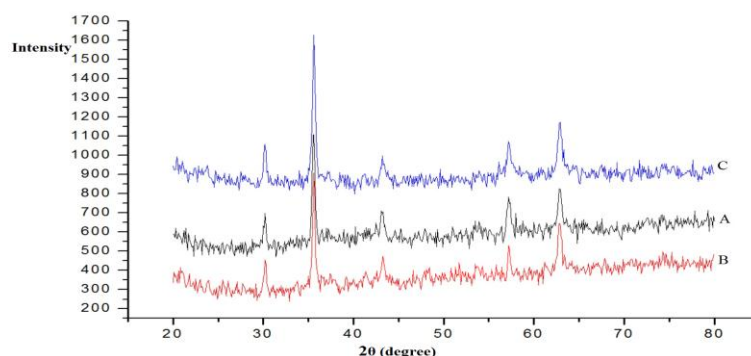
Fig.1: XRD pattern of [(Ni$_{.6}$ Cu$_{.0.2}$ Co$_{0.2}$) Fe$_2$O$_4$] [(Ni$_{.0.2}$ Cu$_{.0.2}$ Co$_{0.6}$) Fe$_2$O$_4$], [(Ni$_{.0.4}$ Cu$_{.0.2}$ Co$_{0.4}$) Fe$_2$O$_4$].
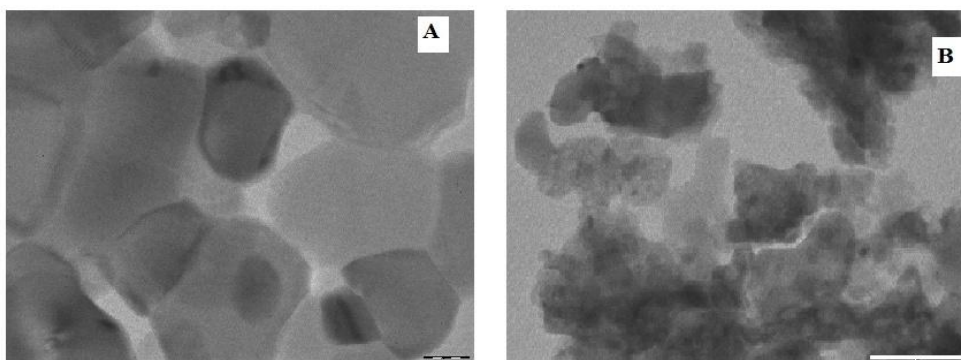
TEM images of typical samples of Ni $_x$ Cu $_{0.2}$ Co $_{0.8-x}$ Fe$_2$O$_4$ for (A) x = 0.2, (B) x= 0.4

Fig.2: TEM images
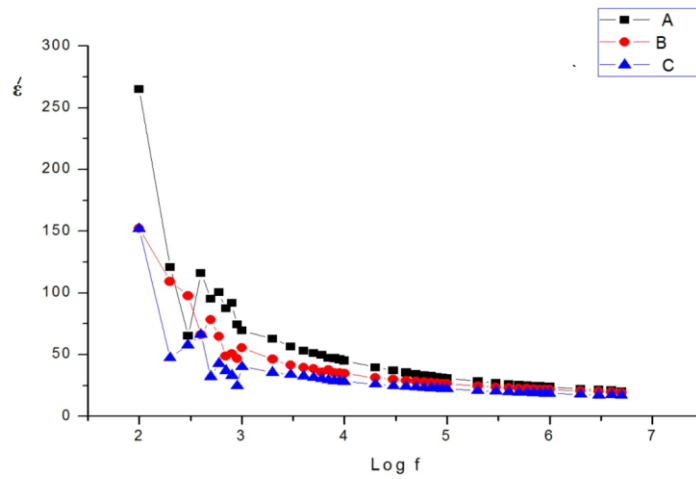
Fig. 3: Variation in dielectric constant (έ) with increase in frequency.
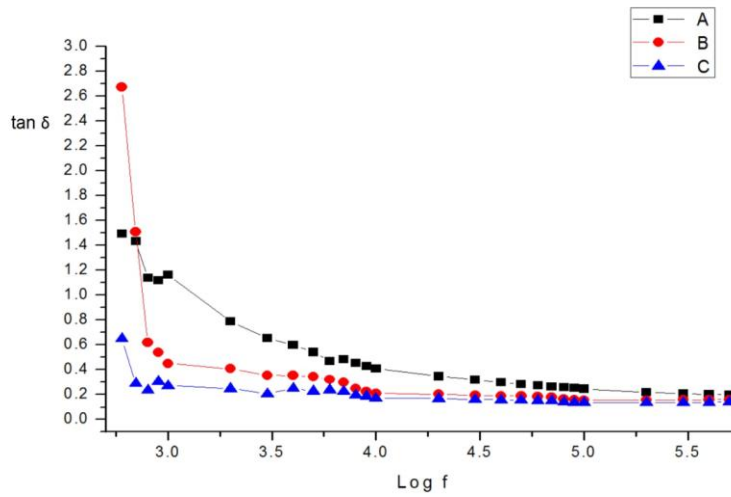
Fig. 4: Variation in dielectric loss (tan δ) with increase in frequency.
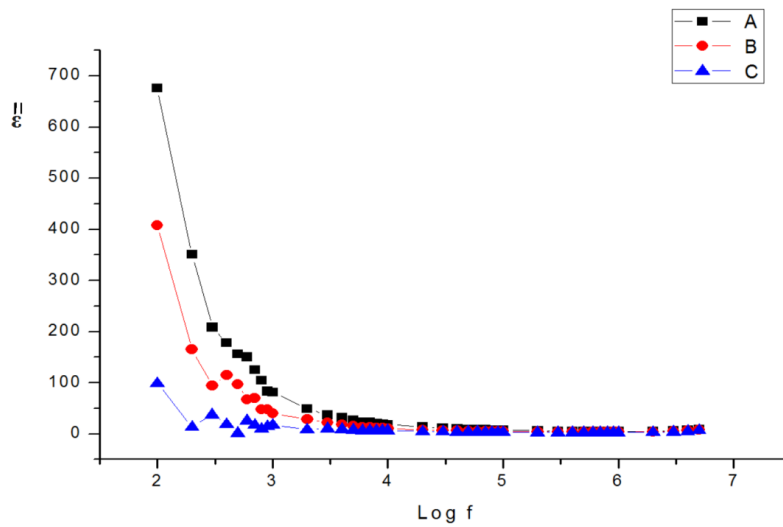
Fig. 5: Variation in Imaginary Part of Dielectric constant (ε″) with increase in frequency.
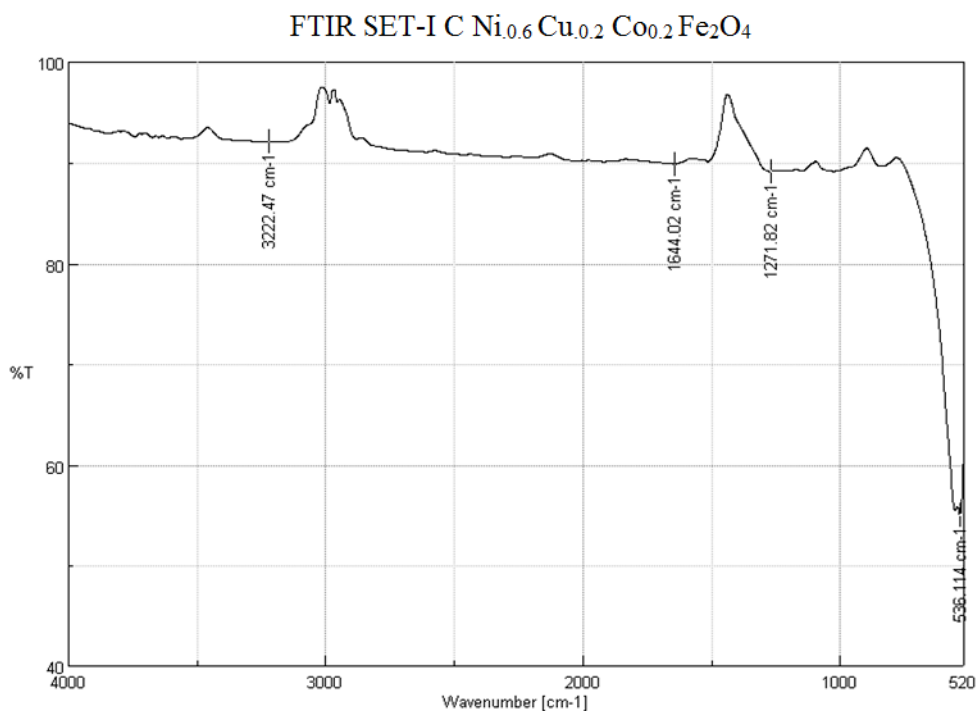
Fig.6: FT-IR spectra of [(Ni$_{.0.6}$Cu$_{.0.2}$Co$_{0.2}$) Fe$_2$O$_4$].

V. Conclusions

The nanocrystalline ferrite samples [(Ni$_{.0.2}$Cu$_{.0.2}$Co$_{0.6}$) Fe$_2$O$_4$], [(Ni$_{.0.4}$Cu$_{.0.2}$Co$_{0.4}$) Fe$_2$O$_4$], [(Ni$_{.0.6}$Cu$_{.0.2}$Co$_{0.2}$) Fe$_2$O$_4$] have been successfully prepared by sol-gel auto combustion technique. All the prepared samples show the single phase cubic spinel structure of the samples. The particle grain size obtained from X-ray diffraction data decreases with increase in Ni^{+2} substitution Cu Co.It clearly shows that the size of the ferrite particles was in the nanometer range. The particle size and nanostructure of the sample was examined by TEM. The particle size calculated from TEM was found to be in close agreement with XRD. Measurement of the dielectric constant and dielectric loss in the 100 Hz–5 MHz frequency range showed higher magnitude, at lower frequencies, decreasing with increase in frequency, essentially becoming constant above 3.5 MHz.

References

[1]. Y.-L. Liu, Z.-M. Liu, Y. Yang, H.-F. Yang, G.-L. Shan, R.-Q. Yu, Simple synthesis of MgFe$_2$O$_4$ as gas sensing materials, Sens. *Actuat. B 107 (2005)* 600–604.
[2]. C.V. Gopal Reddy, S.V. Manorama, V.J. Rao, Preparation and characterization of ferrite as gas sensor materials, *J. Mater. Sci. Lett. 19* (2000) 775.
[3]. N. Xinshu, L. Yanli, X. Jiaqiang, Simple synthesis of MgFe$_2$O$_4$ as gas sensing materials, *Chin. Funct. Mater.* 33 (2002) 413.
[4]. L. Satyanarayana, K. Madhusudan Reddy, V.M. Sankara, Nanocrystalline spinel Ni$_{0.6}$Zn$_{0.4}$Fe$_2$O$_4$: *a novel materials for H$_2$S, Mater. Chem. Phys.* 82 (2003) 21.
[5]. G.F. Goya, H.R. Rechenberg, Superparamagnetic transition and local-order in CuFe$_2$O$_4$ nanoparticles, *Nanostruct. Mater.* 10 (1998) 1001–1011.
[6]. J.Z. Jiang, G.F. Goya, H.R. Rechenberg, Magnetic properties of nanostructured CuFe$_2$O$_4$, *J. Phys. Condens. Mater.* 11 (1999) 4063–4078.
[7]. P.B. Pandya, H.H. Joshi, R.G. Kulkarni, Magnetic and structural properties of CuFe$_2$O$_4$, prepared by co-precipitation method, *J. Mater. Sci. Lett.* 10 (1991) 474–476.
[8]. L.M. Salah, A.M. Moustata, I.S. Ahmed Ferg, Structural characteristics and electrical properties of copper doped manganese ferrite, *Ceram. Int.* 38 (2012) 5605–5611.
[9]. E. VeenaGopalan, I.A. Al-omari, K.A. Malini, P.A. Joy, D. Sathikumar, Y. Yoshida, M.R. Anantharaman, Impact of zinc substitution on the structural and magnetic properties of chemically derived nanosized manganese zinc mixed ferrites, *J. Magn. Magn. Mater.* 321 (2009) 1092–1099.
[10]. Satyendra Singh, B.C. Yadav, Rajiv Prakash, Bharat Bajaj, Synthesis of nanorods and mixed shaped copper ferrite and their applications as liquefied petroleum gas sensor, *Appl. Surf. Sci.* 257 (2011) 10763–10770.
[11]. Satyendra Singh, B.C. Yadav, V.D. Gupta, K. Dwivedi, Investigation on effects of surface morphologies on response of LPG sensor based on nanostructured copper ferrite system, *Mater. Res. Bull.* 47 (2012) 3538–3547.
[12]. Abid Hussain, Tahir Abbas, S.B. Niazi, Preparation of Ni$_1$ $_x$Mn$_x$Fe$_2$O$_4$ ferrites by sol–gel method and study of their cation distribution, *Ceram. Int.* 39 (2013) 1221–1225.
[13]. D.R. Patil, B.K. Chougule, Effect of copper substitution on electrical and magnetic properties of NiFe$_2$O$_4$ ferrite, *Mater. Chem. Phys.* 117 (2009) 35–40.

[14]. A.T.Raghavendar, Damir Pajic, Kreso Zadro, Tomislav Milekovic, P. Vekateshwar Rao, K.M. Jadhav, D. Ravinder, *J. Magn.Magn.Mater.* 3 (2007) 204.
[15]. C. G. Whinfrey, D. W. Eckort and A. Tauber, *J. Am. Chem. Soc.* 53 (1982) 2722
[16]. C. Caizer, M. Stefanescu, *J. Phys. D. Appl. Phys.*35 (2002) 3035.
[17]. M.A. Ahmed, S.F. Mansour, M. Afifi, *J. Magn. Magn. Mater.* 324 (2012) 4-10.
[18]. P.S. Aghav, V.N. Dhage, M.L. Mane, D.R. Shengule, R.G. Dorik, K.M. Jadhav, *Physica B: Cond. Matter.* 406(2011) 4350
[19]. J. Jing, L. Liangchao, X. Feng, *J. Rare Earths* 25 (2007) 79.
[20]. S. Sun, C.B. Murray, D. Weller, L. Folks, A. Moser, Monodisperse FePt nanoparticles and ferromagnetic FePt nanocrystal superlattices, *Science* 287 (2000) 1989.
[21]. I.H. Gul, W. Ahmed, A. Maqsood, Electrical and magnetic characterization of nanocrystalline Ni–Zn ferrite synthesis by co-precipitation route, *J. Magn. Magn. Mater.* 320 (2008) 270–275.
[22]. M.U. Islam, T. Abbas, Shahida B. Niazi, Zubair Ahmad, Sadia Sabeen, M. Ashraf Chaudhry, Electrical behaviour of fine particle co-precipitation prepared Ni–Zn ferrites, *Solid State Commun.* 130 (2004) 353–356.
[23]. J. Smit, H.P.J. Wijn, Ferrites, in: *Phililps Technical Library, Eindhovan, Netherlands*, 1959, pp. 221–245.
[24]. B.D. Cullity, in: *Elements of X-ray Diffraction, second ed., Addison Wesley Pub. Co. Inc.*, 1978.
[25]. A. Verma, R. Chatterjee, Effect of zinc concentration on the structural, electrical and magnetic properties of mixed Mn–Zn and Ni–Zn ferrites synthesized by the citrate precursor technique, *J. Magn. Magn. Mater.* 306 (2006) 313–320.
[26]. T. Nakamura, Y. Okaro, Electromagnetic properties of Mn–Zn ferrite sintered ceramics, *J. Appl. Phys.* 79 (1996) 7129.
[27]. A. Verma, T.C. Geol, R.G. Menditratta, Magnetic properties of nickel–zinc ferrites prepared by the citrate precursor method, *J. Magn. Magn. Mater.* 210 (2000) 274.
[28]. L.G. Van Uitert, DC resistivity in the nickel and nickel zinc ferrite system, *J Chem. Phys.* 23 (10) (1955) 1883.
[29]. C. Heck, in: *Magnetic Materials and their Applications, Butterworths, London,* 1974 506.
[30]. M.R. Anantharaman, S. Sindhu, S. Jagatheesan, K.A. Malini, P. Kurian, Dielectric properties of rubber ferrite composites containing mixed ferrites, *J Phys.* D 32 (1999) 1801.
[31]. T.Jahanbin, M. Hashim, K. A. Mantori, Comparative studies on the structure and electromagnetic properties of Ni-Zn ferrites prepared via co-precipitation and conventional ceramic processing routes, *J. Magn. Magn. Mater.* 322(2010) 2684-2689.
[32]. C.G. Koops, On the dispersion of resistivity and dielectric constant of some semiconductors at audio frequencies, *Phys. Rev.* 83 (1951) 121.
[33]. J S. Upadhyay, S. Devendrakumar, S. Omprakash, Effect of compositional variation on dielectric and electrical properties of Sr$_{1-x}$La$_x$Ti$_{1-x}$Co$_x$O$_3$ system, *Bull. Mater. Sci.* 19 (1996) 513.
[34]. A. Verma, T.C. Goyal, R.G. Menditratta, M.I. Alam, Dielectric properties of NiZn ferrites prepared by the citrate precursor method, *Mater. Sci. Eng.* B60 (1999) 156–162.
[35]. H. Hsiang, W.S. Chen, Y.L. Chang, F.C. Hsu, F.S. Yen, Ferrite load properties of NiZn ferrite powders-epoxy resin coatings, Am. *J. Mater. Sci.* 1 (2011) 40–44.
[36]. K.W. Wagner, *Ann. Phys.* 40 (1913) 817.
[37]. I.T. Rabinkin, Z.I. Novikova, *Ferrites, Izv Acad. Nauk USSR, Minsk,* 1960.
[38]. J.C. Maxwell, Electricity and Magnetism, *vol. 1, Oxford University Press, New York* (1973), p. 1.
[39]. M. Penchal Reddy, W. Madhuri, N. Ramamanoher Reddy, K.V. Siva Kumar, V.R.K. Murthy, R. Ramakrishna Reddy, Influence of copper substitution on magnetic and electrical properties of MgCuZn ferrite prepared by microwave sintering method, *Mater. Sci. Eng.* C 30 (2010) 1094–1099.
[40]. J. Azadmanjiri, H.K. Salehani, M.R. Barati, F. Farzan, Preparation and electromagnetic properties of Ni$_{1-x}$Cu$_x$Fe$_2$O$_4$ nanoparticle ferrites by sol–gel auto-combustion method, *Mater. Lett.* 61 (2007) 84–87.
[41]. J. Du, Z. Liu, W. Wu, Z. Li, B. Han, Y. Huang, Preparation of single-crystal copper ferrite nanorods and nanodisks, *Mater. Res. Bull.* 40 (2005) 928–935.